IEEE Access
Multidisciplinary | Rapid Review | Open Access Journal

Received June 19, 2020, accepted June 30, 2020, date of publication July 13, 2020, date of current version July 30, 2020.

Digital Object Identifier 10.1109/ACCESS.2020.3008901

Feature Extraction and Classification of Lower Limb Motion Based on sEMG Signals

XIN SHI[1,2], PENGJIE QIN[1,2], JIAQING ZHU[1,2], MAQIANG ZHAI[1,2], AND WEIREN SHI[3]

[1]Key Laboratory of Complex System Safety and Control, Ministry of Education, Chongqing 400044, China
[2]Institute of Automation, Chongqing University, Chongqing 400044, China
[3]Shenzhen Institute of Artificial Intelligence and Robotics for Society, Shenzhen 518172, China

Corresponding authors: Xin Shi (shixin@cqu.edu.cn) and Pengjie Qin (qpj_ly@cqu.edu.cn)

This work was supported in part by the National Natural Science Foundation of China (NSFC), China under Project U1613226 and Project U1813217, and in part by the Shenzhen Institute of Artificial Intelligence and Robotics for Society under Project 2019-INT009.

ABSTRACT Surface electromyography (sEMG) signals can reflect the body motion information and are widely used in military, medical rehabilitation, industrial production. The lower limb motion classification mainly includes feature extraction and classification model establishment. Firstly, we proposed a feature extraction method based on the wavelet packet transform (WPT) and principal component analysis (PCA). We used the wavelet packet method to decompose the sEMG signals of three muscles in the lower limb and got the 24-dimensional eigenvector. To reduce the calculation and improve the speed of the classification model, we used the PCA method to reduce the dimension of the feature vector and got the 3-dimensional eigenvector. Then, we proposed a method based on the scale unscented Kalman filter (SUKF) and neural network (NN) for lower limb motion classification. Through the scale correction unscented transform (SCUT) could optimize the neural network weight and improve lower limb motion classification accuracy. Finally, the experimental results showed that the average accuracy was 93.7%. Compared with the backpropagation neural network (BPNN) and wavelet neural network (WNN), this method could improve the accuracy and reliability of the lower limb motion classification.

INDEX TERMS sEMG signals, lower limb motion classification, feature extraction, wavelet packet transform, principal component analysis, unscented Kalman filter, neural networks.

I. INTRODUCTION

The sEMG is the bioelectric signal produced by muscle activity. It contains much information about muscle activity and has the advantages of noninvasive recording [1]. In recent years, it has become a research hotspot in human-machine integrated intelligent equipment [2].

For example, rehabilitation training robots, boosting exoskeleton robots, and intelligent prosthetics [3]–[5]. But, the sEMG classification is very complex because of its nonlinearities and instability [6]. During the motion of the lower limbs, the sEMG is susceptible to interference [7], [8]. It is difficult to extract the feature that can accurately reflect the lower limb motion, and the established classification model is not reliable. Therefore, this paper focuses on the new method of feature extraction and classification model establishment.

The associate editor coordinating the review of this manuscript and approving it for publication was Filbert Juwono.

In the process of the sEMG feature extraction, many researchers used the time or frequency analysis methods to extract feature vectors from sEMG signals [9]–[13]. For example, sEMG amplitude, root mean square (RMS), zero-crossing (ZC), autoregressive-coefficient, mean absolute value (MAV), fourier transform coefficient, cepstrum-coefficients, peak frequency, and median frequency analysis methods [14], [15]. However, the time-domain or frequency-domain analysis can't completely describe the change of the sEMG signal [16]. Recent studies have shown that the time-frequency analysis can extract more sEMG feature information [17]–[19]. Such as C. Sravani proposed flexible analysis wavelet transform(FAWT) to decompose the sEMG signal into 8 sub-bands, and extracted negative entropy, mean absolute value (MAV), variance (VAR), modified mean absolute value type 1 (MAV1), waveform length (WL), simple from the sub-bands features of squared integral (SSI), tsallis entropy, integral electromyography (IEMG) as feature vectors [20]. S. Chada proposed an algorithm

based on the adjustable Q-factor wavelet transform (TQWT), which decomposed the signal into 8 sub-bands features [21]. Xugang Xi proposed a feature extraction method based on a coherence analysis, which used wavelet transform to extract a 32-dimensional wavelet coherence coefficient (WCC) as feature vectors [22]. Although the above research could improve the classification accuracy of the lower limb motion, they generate high-dimensional feature vectors, which easily introduce noise interference and reduce the stability of the model. Therefore, we proposed a feature extraction method based on the wavelet packet transform and PCA to reduce the dimension of feature vectors and extract stable feature vectors. Firstly, the wavelet packet transform was used to extract the energy features, and then the PCA method was used to rank the importance of the feature values to reduce the raw feature vector dimension.

In the process of classification. The sEMG signals have complex nonlinearity, strong coupling, and dynamic time-varying characteristics [23]. Researchers have mainly studied linear discriminant analysis, bayesian networks, neural networks, multilayer perceptrons, fuzzy approximation, support vector machines, fuzzy neural systems, backpropagation neural networks, and wavelet neural network classification methods [24]–[27]. Since the neural network has strong nonlinear approximation performance and the ability to handle unknown internal mechanism problems [28], [29], which is suitable for complex lower limb motion classification. However, in the process of complex lower limb motion classification, the neural network model needs to learn iteratively during the training process, resulting in slow convergence and easily fall into a locally optimal solution. Therefore, the accuracy of the model needs to be improved. In recent years, the unscented Kalman filter is a new filter estimation algorithm, which has been applied by researchers to adaptive control of exoskeleton [30], [31]. Therefore, we applied the UKF algorithm to lower limb motion classification and used the scale correction to improve the UKF filtering accuracy. Hence, we proposed a scale unscented Kalman neural network (SUKFNN) lower limb motion classification method, which improved the stability and classification accuracy.

As far as the author knew, the wavelet packet transforms combined with the PCA feature extraction method and scale unscented Kalman neural network classification method proposed in this paper was the first time applied to the lower limb motion classification.

In this study, we collected the three muscles' sEMG signals and extracted the time-frequency domain features using the wavelet packet. For the raw feature vector, we used the PCA method to extract the stable feature information as the input of the classification model. The traditional feature extraction methods were compared and analyzed through the feature evaluation methods. We proposed a SUKFNN method to establish a lower limb motion classification model to classify five movements. The proposed classification algorithm was also used to compare with the BPNN classification method and the WNN classification method.

FIGURE 1. The biometrics wireless sEMG sensor system.

This paper was organized as follows. The second part described the acquisition of the sEMG signals. The third part introduced a new method for feature extraction. The fourth part introduced the design of the classification model. The fifth part gave the analyzed results. The sixth part gave conclusions and follow-up work.

II. sEMG ACQUISITION

The sEMG signals is a bioelectrical signal recorded from the surface of the human skeletal muscle through surface electromyography electrodes, which is related to neuromuscular activity and contains much information related to limb motion. The different limb movements have different muscle contraction patterns, and the features of myoelectric signals will also be different. By analyzing these features, different movement patterns of the limbs can be distinguished.

We used an sEMG acquisition system developed and manufactured by Biometrics UK to collect sEMG signals, as shown in Figure 1. The sampling frequency was 2000 Hz, and the amplifier's input impedance was greater than 100MOhms. The experimental computing platform processor was Intel(R) Core (TM) i7-9750H CPU@ 2.60GHz, the memory was 16G, and the data analysis software was MATLAB2015b.

We chose five common movements of lower limbs: horizontal walking (HW), crossing obstacles (CO), standing up (SU), downing the stairs (DS), and going up the stairs (GU). The literature [10] showed that medial gastrocnemius (MG) is helpful for walking and running, while lateral femoral muscle (VL) and semitendinosus muscle (ST) has the functions of bending the knee and extending the hip. Therefore, we selected the above three muscles as the source of the myoelectric signal acquisition, as shown in Figure 2.

We used three sEMG sensors to classify five lower limb movements. That were HW, CO, SU, DS, and GU, as shown in Figure 3.

We selected five healthy subjects to participate in the experiment: 23, 23, 25, 26, 24 years old. Their body fat rate for 17 $\pm$ 3% and height for 170 $\pm$ 5 cm. All the healthy subjects performed the above five lower limb movements, and each was cycled in the form of ''relaxation-action-relaxation'' with a completion time for two seconds. The five movement tests were performed for each subject, and each subject tested 500 sets. A total of 2500 sEMG signals were collected to verify the effectiveness of the algorithm.

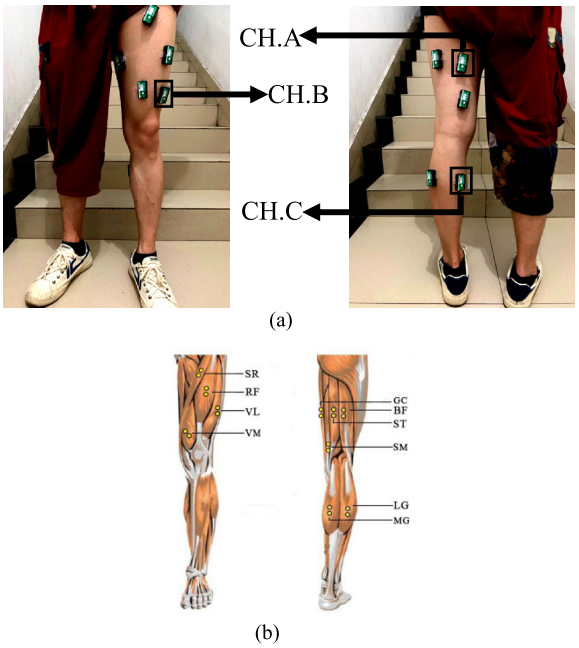

FIGURE 2. The sEMG signal sensor location. The Channel A was located in the thigh semitendinosus (ST), The Channel B was located in the lateral thigh muscle (VL), The Channel C was located in the gastrocnemius (MG).

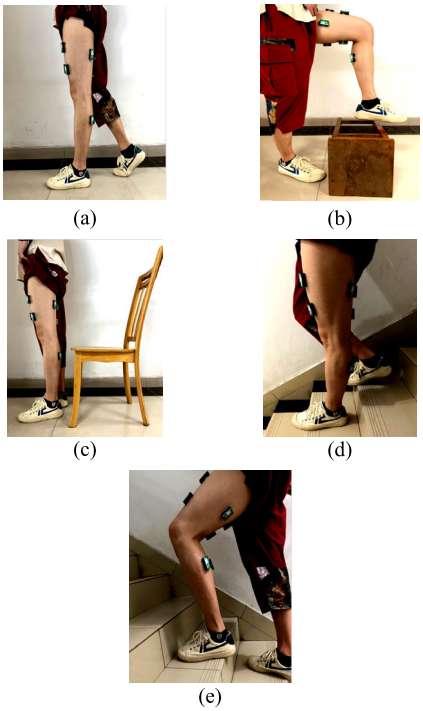

FIGURE 3. The five movements of the lower limb. (a)HW. (b)CO. (c)SU. (d)DS. (e)GU.

III. ALGORITHM DESCRIPTION

We proposed a new feature extraction algorithm based on the wavelet packet transform combined with the PCA method. Firstly, we used energy to extract complex sEMG signals to obtain energy eigenvectors. Then, through the PCA method, the feature vector dimension was reduced. Finally, we proposed an sEMG signal classification method based on a scale unscented Kalman neural network and given the design process of the SUKFNN algorithm.

A. EFFECTIVE FEATURE EXTRACTION

The wavelet analysis only decomposed the low-frequency space but did not decompose the high-frequency interval containing a lot of details. The wavelet packet analysis decomposed the high-frequency part, which could improve the time-frequency resolution.

We used wavelet packet transform to extract sEMG signal features. Firstly, decomposing the raw signal into layer $j(j = 3)$ and get 2^j subspaces of the same bandwidth.

$$s_j^n(t) = \sum_k D_k^{j,n} \Psi_{j,k}(t), \quad k \in Z,\ n = 0, 1, \ldots, 2^{j-1} - 1 \tag{1}$$

where the $D_k^{j,n}$ was wavelet decomposition coefficient of subspace, the $\Psi_{j,k}(t)$ was wavelet basis function, the k was the number of sampling points, and the n was the number of subspaces, as 8. The sum of the squared wavelet packet coefficients in the subspace was the energy of the sub-signal, as $E_n = \sum_k \left| D_k^{j,n} \right|^2$.The sum of the energy of all sub-signals was the total energy of the sEMG signal, as E. The wavelet packet energy P_n was the probability of the energy distribution of the signal in each subspace and as defined as $P_n = E_n/E$. The wavelet packet energy entropy was defined as $WPEE = -\sum_n P_n \ln P_n$. We calculated the wavelet packet energy entropy for different movements to obtain the feature value.

The different wavelet basis functions reflected different characteristics for the sEMG signal. Therefore, we chose a dmey wavelet basis function similar to the raw signal to extract sEMG signal features. The raw signal was shown in Figure 4. We used the dmey basis function to decompose the raw signal into three layers and used three sEMG sensors to obtain a 24-dimensional feature vector. As shown in Figure 5.

We used the wavelet packet decomposition to obtain the sEMG eigenvectors, but some eigenvalues in the vector could not accurately reflect the change of the sEMG signals. If that were brought into the classification model, it would reduce the classification model accuracy. The PCA method could linearly transform a set raw vector into a set vector with fewer eigenvalues. These eigenvalues represented the most relevant information in the raw vectors.

Therefore, we used the PCA method to reduce the redundant information in the raw feature vector and improved the classification model accuracy. As shown in Figure 6, we used the PCA to reduce the three channels' 24-dimensional eigenvectors. According to the PCA method, we ranked the importance of the raw features and selected the top three features to form a 3-dimensional feature vector. Then, we used the 3-dimensional feature vector as the input vector for the classification model.

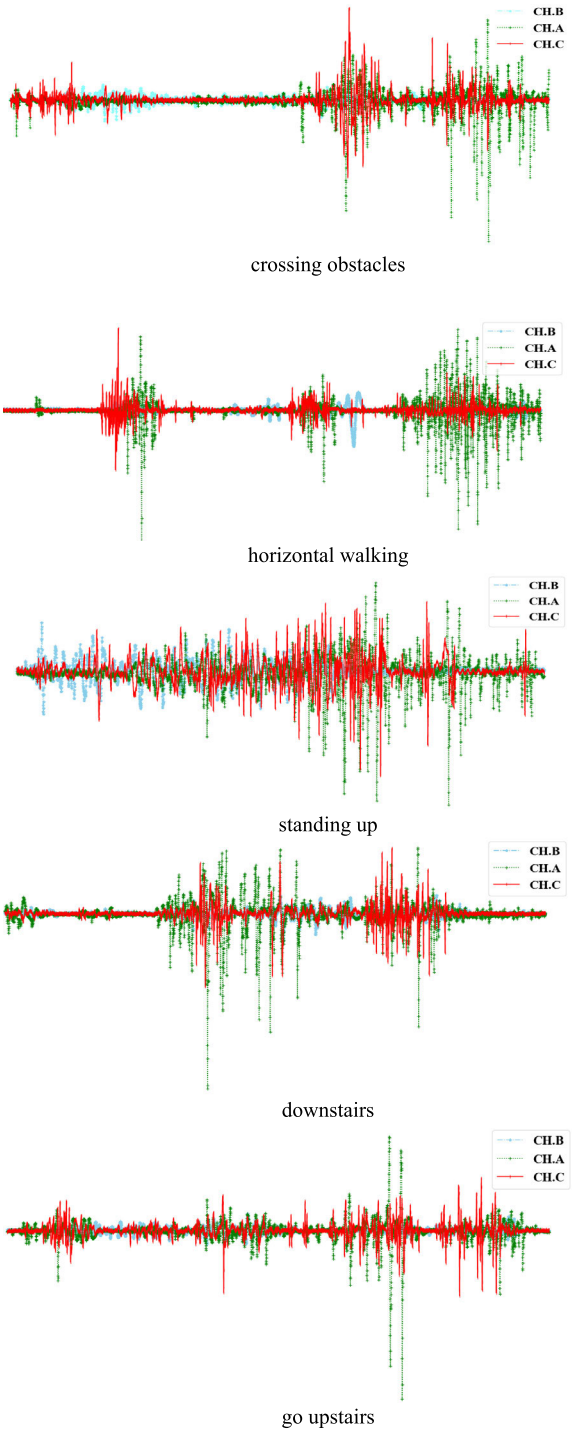

FIGURE 4. The sEMG raw signal, X-axes was the sampling point, Y-axes was the sEMG voltage amplitude.

B. ALGORITHM DESIGN

Since the neural network has a strong nonlinear fitting ability, it is widely used in modeling and optimization of complex nonlinear systems [12], [22], [28]. However, the sEMG signal of the lower limb has complex nonlinearity, strong coupling, and dynamic time-variation, resulting in the lack of stability of the neural network model. In recent years, the hot research

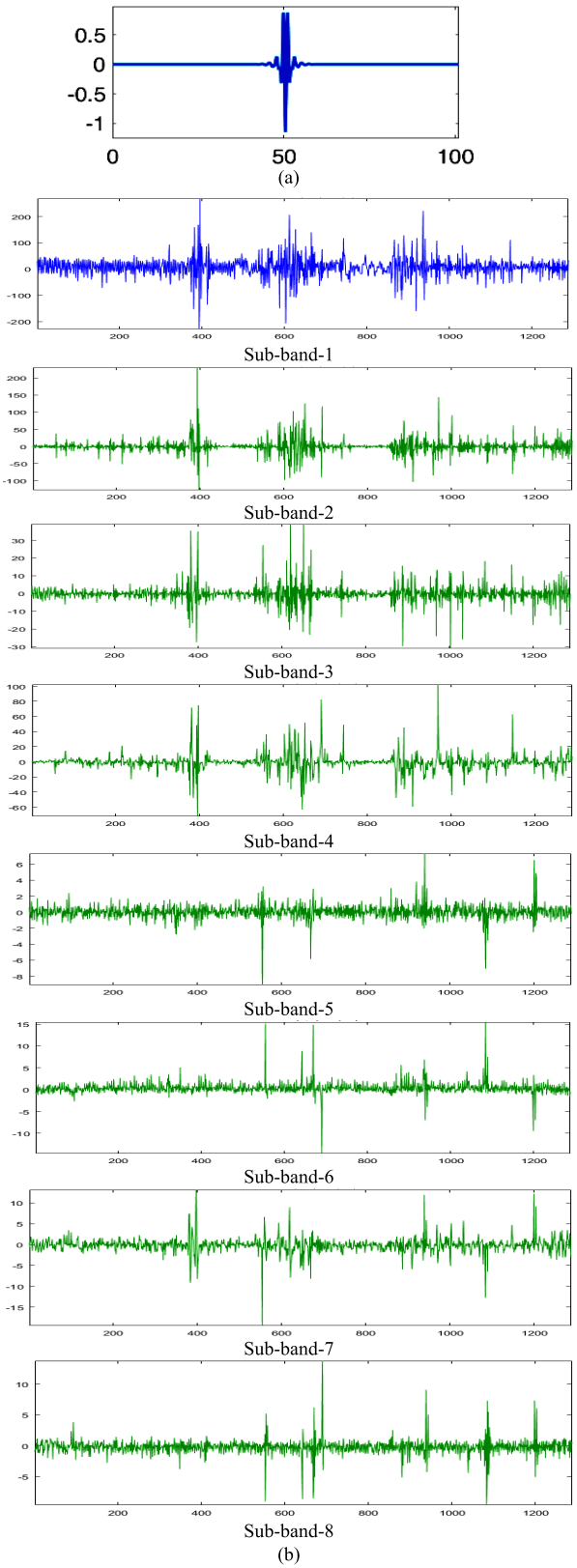

FIGURE 5. Three-layer wavelet packet decomposition feature extraction. (a) The dmey wavelet basis function, X-axes was the sampling point, Y-axes was the signal amplitude. (b) Eight segments of decomposed signals were obtained by three-layer wavelet packet decomposition, X-axes was the sampling point, Y-axes was the sEMG voltage amplitude.

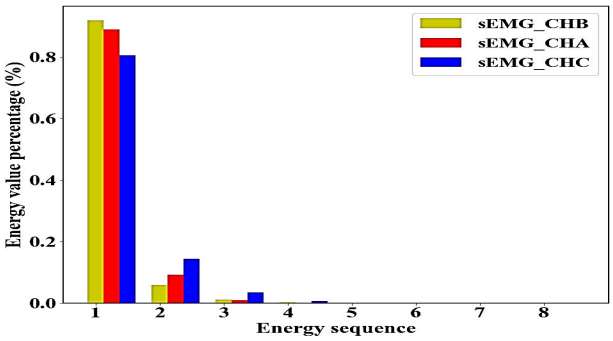

(c)

FIGURE 5. *(Continued.)* **Three-layer wavelet packet decomposition feature extraction. (c) The feature vector of three muscles.**

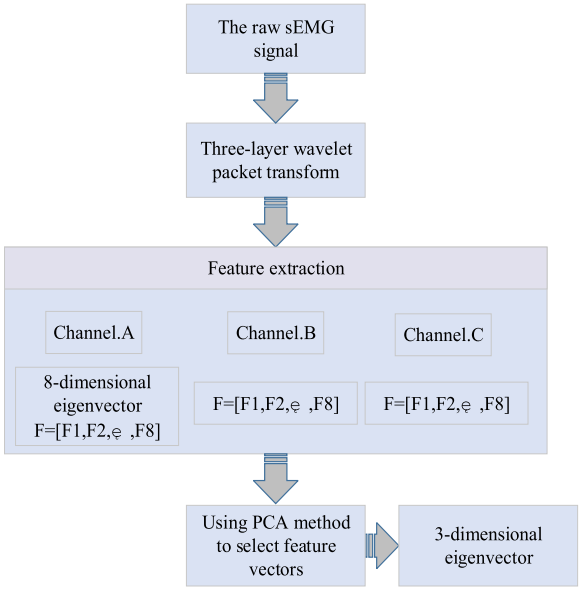

FIGURE 6. **The sEMG feature extraction algorithm flow.**

direction to solve nonlinear estimation is to use the unscented Kalman filter (UKF) algorithm [30], [31]. Therefore, we used the UKF algorithm to dynamically optimize the weights of the neural network, enhancing the adaptive ability and improving the accuracy of the model.

Since the UKF algorithm uses the symmetric sampling strategy, it needs to calculate many sampling points, which is easy to produce non-local effects of sampling. That will lead to low accuracy of neural network weight estimation.

Therefore, we applied the scale modified sampling strategy to symmetric sampling and proposed a scale unscented Kalman neural network (SUKFNN) to improve classification accuracy.

The SUKFNN structure was a three-layer neural network. Where the I is input node of the network, and the O is output node. The l is a constant greater than 1 and less than 10. In the process of the WNN and BPNN classification, the enumeration method was used to determine the training times

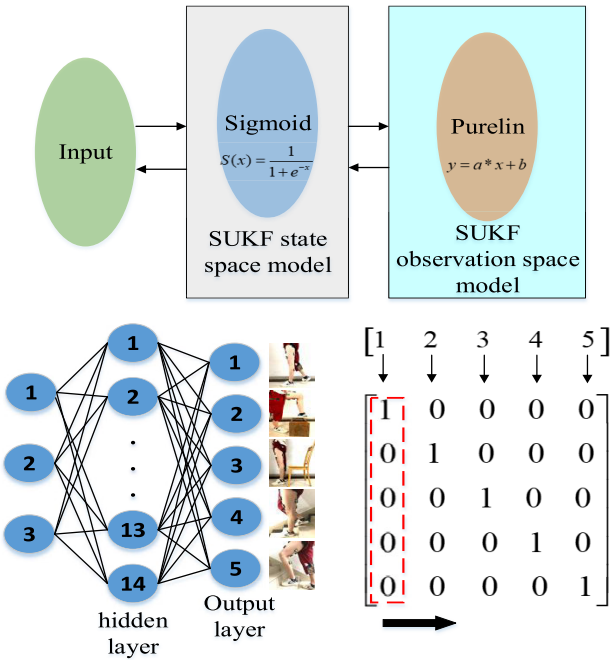

FIGURE 7. **Three-layer SUKF neural network structure.**

were set to 5000, and the learning rate was 0.01, the training error was 0.00, according to equation 2, the node in the hidden layer of the neural network was determined to be 12.

$$H = \sqrt{I + O} + l \tag{2}$$

The transfer function selected by the hidden layer was a nonlinear unipolar excitation function was *Sigmoid*. The output layer transfer function selected a linear function was *Purelin*, which could output an arbitrary value. As shown in Figure 7.

We used the UKF filtering algorithm to correct the three-layer neural network connection weights. The input of the neural network was X, constructing the state equation of the UKF filtering algorithm. The output of the neural network was taken as its measurement equation. Therefore, the state equation and observation equation for the UKF algorithm was:

$$w_{k+1} = w_k + \omega_k \tag{3}$$

$$y_k = f_k(w_k, x_k) + v_k \tag{4}$$

where the w_k was weight, the x_k was input vector, the y_k was output of the neural network. the f_k was transfer function of the neural network. ω_k, v_k were input noise and measurement noise of the neural network. All were obeying the mean value of 0, and the variance was the normal distribution of R^W, R^V.

We assumed that the random variable formed by the weight of the neural network was X. The initialization expectation and covariance were $\overline{X}$ and P_x, respectively. The correction

algorithm as follows:

$$\chi_i = \begin{cases} \overline{X} + (\sqrt{(D+\lambda)P_x})_i, & i = 1, \ldots, D \\ \overline{X} - (\sqrt{(D+\lambda)P_x})_i, & i = D+1, \ldots.., 2D \\ \overline{X}, & i = 0 \end{cases} \quad (5)$$

where the D was dimension of weight and the χ_i defined as *Sigma*. The λ was defined as follows:

$$\lambda = \alpha^2(D+\kappa) - D \quad (6)$$

where the α was a scale factor and could adjust the distance between the *Sigma* and the $\overline{X}$. The value of α was 0.01. The κ was a scaling parameter, set to 0.

Through we proposed a scale sampling correction algorithm, the low filtering accuracy due to the high dimensionality of the state variable was solved.

We designed the steps of the SUKFNN algorithm as follows:

(1) Initializing the neural network weights and covariances.

$$\overline{x}_0 = E[x_0] \quad (7)$$

$$P_o = E[(x_0 - \overline{x}_o)(x_0 - \overline{x}_0)^T] \quad (8)$$

(2) Calculating points set the $\chi_{i,k-1}$ and the weighting parameters ω_i^m, ω_i^c.

$$\chi_{k-1} = \left\lfloor \bar{x}_{k-1}\ \bar{x}_{k-1} + \sqrt{(D+\lambda)}p_{k-1}\ \bar{x}_{k-1} - \sqrt{(D+\lambda)}p_{k-1} \right\rfloor \quad (9)$$

$$\omega_i^m = \begin{cases} \lambda/D+\lambda, & i = 0 \\ 1/2(D+\lambda), & i = 1, \ldots, 2D \end{cases} \quad (10)$$

$$\omega_i^c = \begin{cases} (\lambda/D+\lambda) + 1 - \alpha^2 + \beta, & i = 0 \\ 1/2(D+\lambda), & i = 1, \ldots, 2D \end{cases} \quad (11)$$

Through experimental verification, the value of β was 2.

(3) Updating the time through the state of the neural network and the measurement equation.

$$\chi_{i,k|k-1} = \chi_{i,k-1} \quad (12)$$

$$\overline{x}_{k,k-1} = \sum_{i=0}^{2n} \omega_i^m \chi_{i,k|k-1} \quad (13)$$

$$P_{x_{k,k-1}} = \sum_{i=0}^{2n} \omega_i^c [\chi_{i,k|k-1} - \overline{x}_{i,k|k-1}] \times [\chi_{i,k|k-1} - \overline{x}_{i,k|k-1}]^T + Q_k \quad (14)$$

$$\gamma_{i,k|k-1} = f(\chi_{i,k|k-1}) \quad (15)$$

$$\overline{y}_{k,k-1} = \sum_{i=0}^{2n} \omega_i^m \gamma_{i,k|k-1} \quad (16)$$

(4) Calculating the covariance of the weight variable and the output variable.

$$P_{y_k} = \sum_{i=0}^{2n} \omega_i^c [\gamma_{i,k|k-1} - \overline{y}_{k,k-1}][\gamma_{i,k|k-1} - \overline{y}_{k,k-1}]^T + R_k \quad (17)$$

$$P_{x_{k,y_k}} = \sum_{i=0}^{2n} \omega_i^c [\chi_{i,k|k-1} - \overline{x}_{k,k-1}][\gamma_{i,k|k-1} - \overline{y}_{k,k-1}]^T \quad (18)$$

where the Q_k was covariance of process noise and the R_k was covariance of measurement noise.

$$Q_k = E[\omega_k \omega_k^T] \quad (19)$$

$$R_k = E[v_k v_k^T] \quad (20)$$

(5) Calculating the filter gain.

$$K_k = P_{x_k|y_k} P_{y_k}^{-1} \quad (21)$$

(6) Updating the neural network weight state estimates and covariance.

$$\overline{x}_k = \overline{x}_{k,k-1} + K_k(y_k - \overline{y}_{k,k-1}) \quad (22)$$

$$P_{x_k} = P_{x_{k,k-1}} - K_k P_{y_k} K_k^T \quad (23)$$

We used the UKF filtering algorithm to optimize the neural network weight parameters and proposed a scale correction algorithm to solve the UKF filtering divergence problem caused by the high dimensional features.

IV. RESULTS

We compared the mean value (MAV), root mean square (RMS), wavelet transform coefficient (WTC), and the improved wavelet packet transform. The MAV, RMS and WTC were popular methods for sEMG feature extraction [14], [15], [17]–[19].

In the time domain, the sEMG could be approximated as a random signal with a mean value of 0. The mean absolute value (MAV) was defined as:

$$MAV = \frac{1}{N}\sum_{i=1}^{N} |x_i|, \quad i = 1, 2, 3, \ldots, N \quad (24)$$

where the x_i was sample data, the N was sample length, which was 4000.

We calculated the MAV eigenvalues for the three muscles to obtain 3-dimensional eigenvectors.

The root mean square (RMS) was a typical feature parameter in the time domain analysis. It was used to measure the trend for SEMG signals. The root mean square was defined as:

$$RMS = \sqrt{\frac{1}{N}\sum_{i=1}^{N} x_i^2}, \quad i = 1, 2, 3, \ldots, N \quad (25)$$

where the x_i was sample data, the N was the sample length, which was 4000.

We calculated the RMS eigenvalues for the three muscles to obtain 3-dimensional eigenvectors.

The wavelet transforms coefficient (WTC) is a time-frequency analysis method. Xugang Xi decomposed the raw signal into five-layers and selected the maximum wavelet coefficient as the sEMG signal feature [22].

$$WTC_j = \sqrt{\frac{1}{K}\sum_{k=1}^{K} W_{j,k}^2} \quad (26)$$

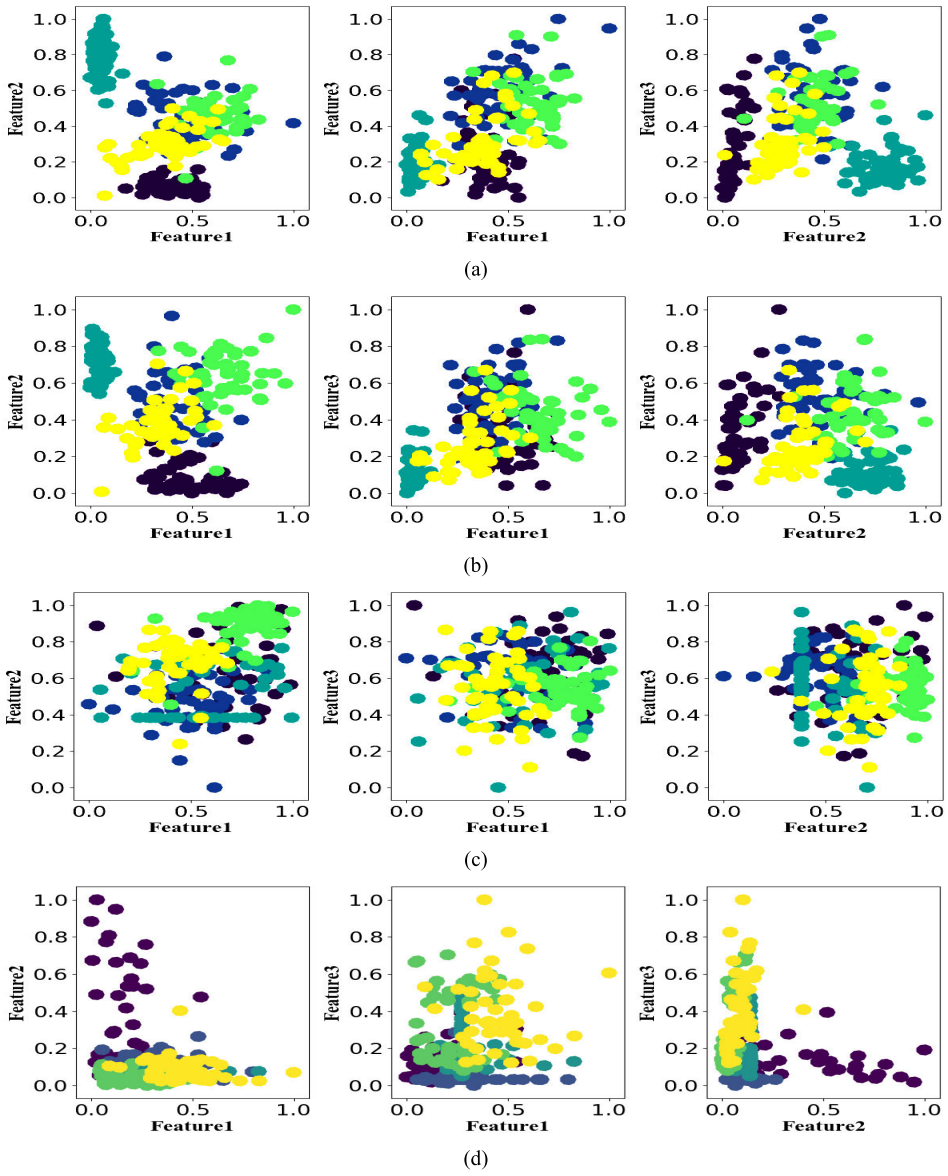

FIGURE 8. (a) Scatter plot for five different motion features extracted using the wavelet packet and PCA. (b) Scatter plot for five different motion features extracted using the MAV. (c) Scatter plot for five different motion features extracted using the RMS. (d) Scatter plot for five different motion features extracted using the WTC.

where the WTC_j is the coefficient of wavelet energies. The K is the number of the j-th layer decomposed coefficient. The $W_{j,k}$ is the k-th coefficient of the j-th layer decomposed coefficient.

We calculated the WTC eigenvalues for the three muscles to obtain 3-dimensional eigenvectors.

A. EVALUATION OF WAVELET PACKET COMBINED WITH PCA METHOD FOR FEATURE EXTRACTION

Figure 8(a) was an sEMG feature scatter plot using an improved wavelet packet feature extraction method. The results were compared with the scatter plot for the RMS (Figure 8(b)), the MAV (Figure 8(c)), and the WTC (Figure 8(d)). Figure 8(a) has the best performance.

The Euclidean distance (ED) was used to measure the distance for sample features. The longer the distance, the greater the difference between sample features. The Standard deviation (SD) was used to measure the dispersion for sample features. The smaller the standard deviation, the more stable the sample features. When the ED value was high, and the SD value was low, we could extract the best feature value.

We used the ratio between ED and SD that we called RES index as a feature statistic measured metrics. The $ED(m, n)$ was defined as

$$ED(m, n) = \sqrt{(m_1 - n_1)^2 + (m_2 - n_2)^2} \tag{27}$$

TABLE 1. Statistical metrics for feature extraction algorithms.

Algorithm	Feature Algorithm Metrics								
	Average Standard deviation (SD)			Euclidean distance (ED)			The ratio between ED and SD (RES)		
	Feature1	Feature2	Feature3	Feature1	Feature2	Feature3	Feature1	Feature2	Feature3
WPT and PCA	9.01	5.55	7.206	59.66	53.59	48.57	6.82	9.65	6.74
MAV	7.64	6.38	5.63	51.81	37.9221	40.58	6.77	5.92	6.59
RMS	22.57	11.21	12.69	84.85	67.31	60.62	3.75	6.01	4.77
WTC	6.89	6.13	7.57	46.1	38.06	50.26	6.69	6.21	6.64

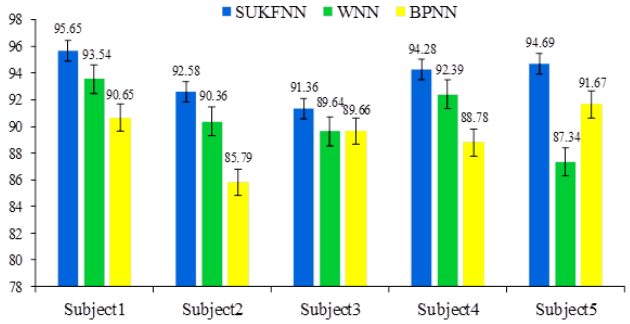

FIGURE 9. The classification accuracy for the different algorithms.

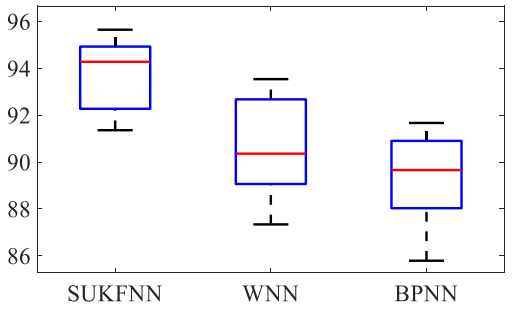

FIGURE 10. Box plot of the classification model.

where the m and n represented two of the three feature sets. The SD was defined as

$$SD = \sqrt{\frac{\sum_{w=1}^{N_W} (r_w - \sigma)^2}{N_W}} \tag{28}$$

where the r_w represented eigenvalue and the N_W represented feature set size ($N_W = 50$). The RES index was defined as

$$RES(m, n) = \frac{ED(m, n)}{SD} \tag{29}$$

Also, we standardized the features. Then calculated the RES index. The normalization for features F_{norm} was performed, it was defined as:

$$F_{norm} = \frac{F + \min(F)}{\max(F + \min(F))} \tag{30}$$

The results showed that the RES index of the WPT combined with PCA was 6.82, 9.65, and 6.74, respectively, which was higher than RMS, MAV, and WTC methods, proved that the improved WPT has the best class separability.

B. RESULTS ANALYSIS

We collected sEMG signals of the three muscles in the lower limbs of five healthy subjects. That was divided that into training samples and testing samples, which were 2000 and 500 samples, respectively. We trained three models with 2000 samples and selected 100 testing samples of each subject to verify the accuracy of five lower limb movements.

Since the WNN and BPNN were common methods of the sEMG signal recognition research [24], [26], [27], We used the WNN and BPNN to classify the five movements of the lower limb. The classification accuracy was shown in Figure 9. The SUKFNN model average accuracy was 93.7%. The WNN model average accuracy was 90.7%. The BPNN model average accuracy was 89.3%. The minimum accuracy of the SUKFNN model was 91.36%, the WNN model was 87.34%, and the BPNN model was 85.79%. It was proved that the SUKFNN model average accuracy was higher than the WNN model and BPNN model.

TABLE 2. Average accuracy rate and standard deviations for three models.

Classification algorithm	Average accuracy rate (%)	Metrics Standard deviation	Running time(s)
SUKFNN	93.71	1.72	0.474
WNN	90.65	2.42	0.585
BPNN	89.31	2.24	0.874

We plotted a box diagram to visually describe the model accuracy, as shown in Figure 10. The results showed that the SUKFNN accuracy was higher than WNN and BPNN. The dispersion for SUKFNN was lower than WNN and BPNN. It was proved that the SUKFNN model has high stability.

Also, the robustness and real-time was an important metric to evaluate the performance for the algorithm, so we calculated the standard deviation, average accuracy, and computational cost according to the results in Figure 9. Table 2 that the SUKFNN was more stable than the BPNN and WNN. The classifier SUKFNN with WPT features resulted in the calculation time below 500ms.

The confusion matrix was an important method to evaluate the accuracy and reliability, which could help us understand the classification performance. The classifier with a low false-positive rate could avoid falling due to the wrong classification of the motion, which was helpful to enhance the practicability and safety of the exoskeleton. This paper selected 1500 testing samples to calculate the confusion matrix for the three algorithms and verified the proposed method's

TABLE 3. SUKFNN model confusion matrix.

Expected motion	Real motion HW	CO	SU	GU	DS
HW	90.5%	—	—	6.3%	3.2%
CO	1.7%	93.2%	—	5.1%	—
SU	—	2.1%	96.8%	0.4%	0.7%
GU	—	3.5%	0.1%	96.1%	0.3%
DS	2%	0.9%	4.2%	—	92.9%

TABLE 4. WNN model confusion matrix.

Expected motion	Real motion HW	CO	SU	GU	DS
HW	91.3%	—	1.2%	4.5%	3%
CO	0.9%	90.6%	1.8%	6.1%	0.6%
SU	—	4.5%	88.7%	4.6%	2.2%
GU	—	3.8%	0.3%	94.6%	1.3%
DS	1.4%	1.6%	5.5%	—	91.5%

TABLE 5. BPNN model confusion matrix.

Expected motion	Real motion HW	CO	SU	GU	DS
HW	87.6%	1.1%	1.5%	5.4%	4.4%
CO	1.9%	90.8%	0.6%	5.4%	1.3%
SU	—	4.7%	89.6%	3.3%	2.4%
GU	0.3%	5.4%	—	91.8%	2.5%
DS	0.2%	1.8%	8.7%	0.4%	88.9%

TABLE 6. Sensitivity metrics of the three Models.

Classification algorithm	Sensitivity HW	CO	SU	GU	DS
SUKFNN	90%	93%	95%	96%	93%
WNN	91%	90%	89%	94%	91%
BPNN	88%	91%	90%	92%	89%

advanced nature. Table 3 showed the confusion matrix for the SUKFNN model. The classification accuracy of horizontal walking (HW) was the lowest, being 90.5%. The false-positive rate was 6.3%. Table 4 showed the confusion matrix for the WNN model. The accuracy for motion classification of the standing up (SU) was the lowest, being 88.7%. The false-positive rate was 4.6%. Table 5 showed the confusion matrix for the BPNN model. The accuracy for the horizontal walking (HW) was the lowest, being 87.6%. It was easy to misjudge the motion for the walking upstairs (GU), and the false-positive rate was 5.4%. Also, the false-positive rate for the SUKFNN model was lower than the WNN model and BPNN model. It was proved that the algorithm proposed in this paper has high accuracy and reliability.

The sensitivity metrics was an important parameter to evaluate reliability. We selected 1200 testing samples to verify the sensitivity of the three models. Table 6 showed the sensitivity metrics for the SUKFNN model, WNN model, and BPNN model. The SUKFNN model has higher sensitivity. It was proved that the SUKFNN model has a lower false-positive rate and better reliability than the WNN model and BPNN model.

Furthermore, we selected a female subject with a height of 155cm and an age of 25 years. Then we collected 100 samples as the testing samples. Because of the difference between the new subjects and the five subjects, the accuracy of the new subjects was lower than the five subjects. However, the overall accuracy of the SUKFNN was still better than WNN and BPNN. As shown in Table 7.

TABLE 7. Classification results of the three models.

Classification algorithm	HW	CO	SU	GU	DS	AC
SUKFNN	85%	90%	95%	90%	90%	90%
WNN	85%	85%	80%	90%	90%	86%
BPNN	75%	80%	80%	85%	85%	81%

We compared the results to demonstrate the effectiveness of our algorithm, as shown in Table 8. In these studies, most researchers used more sEMG sensors to classify lower extremity motions. From Table 8 that at least four muscle sEMG signals need to be acquired to classify five lower limb motions. However, we only need three sensors to classify five lower limb motions, and the accuracy reaches 93.7%.

V. DISCUSSION

In this paper, we proposed the feature extraction method based on the improved wavelet packet transform and a lower limb motion classification method based on SUKFNN. As far as the author knew, this algorithm was the first time applied to the lower limb motion classification.

In many studies, the lower limb motion classification accuracy was improved by increasing the number of electrodes [7], [9], [11], [13], [14], [29]. However, in the actual lower limb movement process, the sEMG sensor will be disturbed by noise, the more sensors will lead to the instability for classification accuracy, and the wearer will also feel uncomfortable. Secondly, with the increase in the number of electrodes, more data dimensions must be processed, and the calculation will increase. Therefore, this paper collected three muscle sEMG signals in the lower limb, which was in accord with the typical lower limb exoskeleton application.

Most studies have classified more than three different movements of the lower limbs and achieved an accuracy of 86%∼95%. In this paper, we used three sEMG sensors to classification five lower limb movements, and the accuracy could reach 93.7%. Since the complexity in sEMG signal calculation, the accuracy and reliability will have an important impact on the practicability for the lower limb exoskeleton. In this paper, the SUKF filtering algorithm was used to estimate the weight of the neural network, which solved the slow convergence speed and easily fell into local optimal value. Also improving the adaptive ability of the model.

The advantages of the proposed method were verified offline. In the future, this method can classify various movements for lower limbs online. Considering the algorithm's application in the exoskeleton, we first set the online acquisition time to obtain the sEMG signal. Then the raw signal features were extracted, and the classification results were given by classifier. Finally, the classifier's results were inputted the controller as control signals, and the exoskeleton performs corresponding actions according to the control signals. Among them, from feature extraction to classification, the computational cost does not exceed 500ms, as shown

TABLE 8. This paper proposed a comparison of lower limb motion classification algorithms with other classification methods.

Author	Number of myoelectric sensors	Types of motion	Methods	Accuracy rate (%)	References
Jinghan Hao et al.	5	5	2-stream hidden Markov model (HMM)	90.17	11
Diana C. Toledo-Pérez et al.	4	6	PCA and SVM	90.12	7
ARVIND GAUTAM et al.	4	3	Long-term Recurrent Convolution Network (LRCN)	92.4	9
Rohit Gupta et al.	2	3	LDA	89.5	13
FANG PENG et al.	4	2	Kernel LDA	92.5	29
Qingsong Ai et al.	4	5	WT and SVM	86.2	14
Propose method	3	5	WPT, PCA, and SUKFNN	93.7	This work

in Table 2. To prove that this method was suitable for more people, the next study will analyze the influence of different age and gender on the classification accuracy.

Also, the interference to the environment noise (electrode deviation and power frequency interference) and muscle fatigue can be considered in practical application to verify the algorithm's autonomous learning and model adjustment ability.

VI. CONCLUSION

We proposed a method for lower limb motion classification based on improved wavelet packet transform and scale unscented Kalman neural network. Firstly, the wavelet packet transform was used to extract the energy features of the sEMG signal from the three channels, and the feature was reduced by the PCA method. Then we proposed a scale unscented Kalman neural network to classify five movements of the lower limb. We proposed a RES feature extraction evaluation method, compared with traditional feature extraction methods, which proved that we proposed the wavelet packet combined with the PCA feature extraction method has better feature correlation and separability. Experimental results showed that the SUKFNN had achieved excellent performance, the model has a low false-positive rate, and the average classification accuracy was 93.7%. Its stability and accuracy are higher than WNN and BPNN algorithms, which proved that the method is advanced, reliable, and practical. This study is beneficial to the widespread application of exoskeleton robots in daily life. Also, in future research, we can increase the diversity of lower limb movements and improve the accuracy of lower limb movement classification.

REFERENCES

[1] Y. Du, H. Wang, S. Qiu, W. Yao, P. Xie, and X. Chen, "An advanced adaptive control of lower limb rehabilitation robot," *Frontiers Robot. AI*, vol. 5, p. 116, Oct. 2018.

[2] W. Yu, W. Ma, Y. Feng, R. Wang, K. Madani, and C. Sabourin, "Generating human-like velocity-adapted jumping gait from sEMG signals for bionic Leg's control," *J. Sensors*, vol. 2017, pp. 1–18, Jan. 2017.

[3] X. Zhang, J. Li, S. E. Ovur, Z. Chen, X. Li, Z. Hu, and Y. Hu, "Novel design and adaptive fuzzy control of a lower-limb elderly rehabilitation," *Electronics*, vol. 9, no. 2, p. 343, Feb. 2020.

[4] Z. Song, C. Tian, and J. S. Dai, "Mechanism design and analysis of a proposed wheelchair-exoskeleton hybrid robot for assisting human movement," *Mech. Sci.*, vol. 10, no. 1, pp. 11–24, Jan. 2019.

[5] J. Deng, P. Wang, M. Li, W. Guo, F. Zha, and X. Wang, "Structure design of active power-assist lower limb exoskeleton APAL robot," *Adv. Mech. Eng.*, vol. 9, no. 11, Nov. 2017, Art. no. 168781401773579.

[6] X. Xi, M. Tang, and Z. Luo, "Feature-level fusion of surface electromyography for activity monitoring," *Sensors*, vol. 18, no. 2, p. 614, Feb. 2018.

[7] D. Toledo-Pérez, M. Martínez-Prado, R. Gómez-Loenzo, W. Paredes-García, and J. Rodríguez-Reséndiz, "A study of movement classification of the lower limb based on up to 4-EMG channels," *Electronics*, vol. 8, no. 3, p. 259, Feb. 2019.

[8] T. Khan, L. E. Lundgren, E. Järpe, M. C. Olsson, and P. Viberg, "A novel method for classification of running fatigue using change-point segmentation," *Sensors*, vol. 19, no. 21, p. 4729, Oct. 2019.

[9] A. Gautam, M. Panwar, D. Biswas, A. Acharyya, "MyoNet: A transfer-learning-based LRCN for lower limb movement recognition and knee joint angle prediction for remote monitoring of rehabilitation progress from sEMG," *IEEE J. Transl. Eng. Health Med.*, vol. 8, 2020, Art. no. 2100310.

[10] S. Kyeong, W. Shin, M. Yang, U. Heo, J.-R. Feng, and J. Kim, "Recognition of walking environments and gait period by surface electromyography," *Frontiers Inf. Technol. Electron. Eng.*, vol. 20, no. 3, pp. 342–352, Mar. 2019.

[11] J. Hao, P. Yang, L. Chen, and Y. Geng, "A gait patterns recognition approach based on surface electromyography and three-axis acceleration signals," *IOP Conf. Ser, Mater. Sci. Eng.*, vol. 533, May 2019, Art. no. 012060.

[12] Y. Li, Q. Zhang, N. Zeng, M. Du, and Q. Zhang, "Prediction of knee joint moment by surface electromyography of the antagonistic and agonistic muscle pairs," *IEEE Access*, vol. 7, pp. 82320–82328, 2019.

[13] R. Gupta and R. Agarwal, "Electromyographic signal-driven continuous locomotion mode identification module design for lower limb prosthesis control," *Arabian J. Sci. Eng.*, vol. 43, no. 12, pp. 7817–7835, Dec. 2018.

[14] Q. Ai, Y. Zhang, W. Qi, Q. Liu, and A. K. Chen, "Research on lower limb motion recognition based on fusion of sEMG and accelerometer signals," *Symmetry*, vol. 9, no. 8, p. 147, Aug. 2017.

[15] X. Xi, M. Tang, S. M. Miran, and Z. Luo, "Evaluation of feature extraction and recognition for activity monitoring and fall detection based on wearable sEMG sensors," *Sensors*, vol. 17, no. 6, p. 1229, May 2017.

[16] J. Yang and C. Peng, "Evolving control of human-exoskeleton system using Gaussian process with local model," *Biomed. Signal Process. Control*, vol. 58, Apr. 2020, Art. no. 101844.

[17] W. Li, Z. Li, S. Qie, H. Yang, X. Chen, Y. Liu, Z. Li, and K. Zhang, "Analysis of the activation modalities of the lower limb muscles during walking," *Technol. Health Care*, pp. 1–12, Jan. 2020.

[18] W. Wang, K. Li, S. Yue, C. Yin, and N. Wei, "Associations between lower-limb muscle activation and knee flexion in post-stroke individuals: A study on the stance-to-swing phases of gait," *PLoS ONE*, vol. 12, no. 9, Sep. 2017, Art. no. e0183865.

[19] A. L. Delis, J. L. A. Carvalho, A. F. da Rocha, R. U. Ferreira, S. S. Rodrigues, and G. A Borges, "Estimation of the knee joint angle from surface electromyographic signals for active control of leg prostheses," *Physiolog. Meas.*, vol. 30, no. 9, pp. 931–946, 2009.

[20] C. Sravani, V. Bajaj, S. Taran, and A. Sengur, "Flexible analytic wavelet transform based features for physical action identification using sEMG signals," *IRBM*, vol. 41, no. 1, pp. 18–22, Feb. 2020.
[21] S. Chada, S. Taran, and V. Bajaj, "An efficient approach for physical actions classification using surface EMG signals," *Health Inf. Sci. Syst.*, vol. 8, no. 1, p. 3, Dec. 2020.
[22] X. Xi, C. Yang, J. Shi, Z. Luo, and Y.-B. Zhao, "Surface electromyography-based daily activity recognition using wavelet coherence coefficient and support vector machine," *Neural Process. Lett.*, vol. 50, no. 3, pp. 2265–2280, Dec. 2019.
[23] Y. M. Aung and A. Al-Jumaily, "sEMG based ANN for shoulder angle prediction," *Procedia Eng.*, vol. 41, pp. 1009–1015, Jan. 2012.
[24] L. Tong, F. Zhang, Z.-G. Hou, W. Wang, and L. Peng, "Bp–Ar-based human joint angle estimation using multi-channel sEMG," *Int. J. Robot. Autom.*, vol. 30, no. 3, pp. 227–237, 2015.
[25] N. Sae Jong and P. Phukpattaranont, "A speech recognition system based on electromyography for the rehabilitation of dysarthric patients: A thai syllable study," *Biocybern. Biomed. Eng.*, vol. 39, no. 1, pp. 234–245, Jan. 2019.
[26] C. Yang, X. Xi, S. Chen, S. M. Miran, X. Hua, and Z. Luo, "SEMG-based multifeatures and predictive model for knee-joint-angle estimation," *AIP Adv.*, vol. 9, no. 9, Sep. 2019, Art. no. 095042.
[27] R. H. Fereydooni, H. Siahkali, H. A. Shayanfar, and A. H. Mazinan, "SEMG-based variable impedance control of lower-limb rehabilitation robot using wavelet neural network and model reference adaptive control," *Ind. Robot, Int. J. Robot. Res. Appl.*, vol. 47, no. 3, pp. 349–358, Jan. 2020.
[28] R. Gupta and R. Agarwal, "Single muscle surface EMGs locomotion identification module for prosthesis control," *Neurophysiology*, vol. 51, no. 3, pp. 191–208, May 2019.
[29] F. Peng, W. Peng, C. Zhang, and D. Zhong, "IoT assisted kernel linear discriminant analysis based gait phase detection algorithm for walking with cognitive tasks," *IEEE Access*, vol. 7, pp. 68240–68249, 2019.
[30] D. R. Bueno and L. Montano, "Neuromusculoskeletal model self-calibration for on-line sequential Bayesian moment estimation," *J. Neural Eng.*, vol. 14, no. 2, Apr. 2017, Art. no. 026011.
[31] Q. Ding, J. Han, and X. Zhao, "Continuous estimation of human multi-joint angles from sEMG using a state-space model," *IEEE Trans. Neural Syst. Rehabil. Eng.*, vol. 25, no. 9, pp. 1518–1528, Sep. 2017.

XIN SHI received the B.Sc., M.Sc., and Ph.D. degrees from Chongqing University, Chongqing, China, in 2000, 2003, and 2010, respectively. He is currently a Professor with the College of Automation, Chongqing University. His main research interests include intelligent information processing and robot intelligent systems.

PENGJIE QIN received the bachelor's degree from the Chongqing Institute of Technology, in 2015. He is currently pursuing the Ph.D. degree with the School of Automation, Chongqing University. His main research interests include signal processing, intelligent systems, and pattern recognition.

JIAQING ZHU received the B.Sc. degree from the North University of China, in 2013. He is currently pursuing the M.Sc. degree with Chongqing University. His main research interests include artificial intelligence and human–machine fusion.

MAQIANG ZHAI received the B.Sc. degree from the Hubei University of Arts and Science, in 2018. He is currently a Graduate Student at Chongqing University. His main research interests include intelligent information processing and complex system modeling.

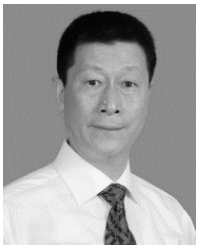

WEIREN SHI is currently a Professor at Chongqing University, and also a Researcher at the Robotics and Intelligent Manufacturing Research Institute, The Chinese University of Hong Kong (Shenzhen). He is a Fellow of the Chinese Instrumentation Society